Tunable investigation optical, electrical and magnetic behaviors of Gd 3+ substituted lanthanum strontium manganite La 0.5-x Sr 0.5 Gd x MnO 3 nanopowders facilely synthesized through citrate precursor technique

Ali Omar Turky, Mohamed M. Rashad, Ali M. Hassan, Elsayed M. Elnaggar, Hailei Zhao, Mikhael Bechelany

Tunable investigation optical, electrical and magnetic behaviors of Gd^{3+} substituted lanthanum strontium manganite $La_{0.5-x}Sr_{0.5}Gd_xMnO_3$nanopowders facilely synthesized through citrate precursor technique

Ali Omar Turky*[abc], Mohamed. M. Rashad[a], Ali M. Hassan[d], Elsayed M. Elnaggar[d], Hailei Zhao[b] , Mikhael Bechelany[c]

[a]Central Metallurgical Research & Development Institute, P.O. Box: 87 Helwan, Cairo, Egypt

[b] Department of Inorganic Nonmetallic Materials, University of Science and Technology Beijing, Beijing 100083, China

[c]Institut Européen des Membranes, IEM UMR-5635, Université de Montpellier, ENSCM, CNRS, Place Eugène Bataillon, 34095 Montpellier cedex 5, France

[d]Faculty of Science, Chemistry department, Al-Azhar University, Nasar City , Egypt,

Corresponding author: ali_omar155@yahoo.com

Abstract

In this report, gadolinium-substituted lanthanum strontium manganite (LSM) system, $La_{0.5}Sr_{0.5-x}Gd_xMnO_3$ ($0.1 \leqslant x \leqslant 0.4$), was synthesized using the citrate precursor processing. The influence of Gd^{3+} ions content on the structure, optical, electrochemical and magnetic properties of LSM was studied. Evidently, in all compositions, a single monoclinic perovskite phase was obtained after calcination at 1000 °C for 2 h. All powders exhibited crystallite sizes in the range of 25.6-35.1 nm. The formed LSM nanopowders has great optical reflectance of 20–40 % from 200 to 800 nm for all substituted samples by Gd^{3+} ions. Furthermore, the LSM possesses good optical absorbance of 0.65 from 200 to 800 nm. The optical band gap energy was decreased from 2.45 to 1.63 eV by increasing the Gd^{3+} ions molar ratios from 0.1 to 0.4.. Meanwhile, the electrochemical impedance spectroscopy displayed the good results. The ohmic resistance (*R*s) and the polarization resistance (*R*p) of the electrode were increased by increasing the Gd^{3+} ions concentration from 0.1 to 0.4. Otherwise, both the ohmic resistance

(*R*s) and polarization resistance in the doped samples were higher than the pure LSM sample. Finally, the saturation magnetization was increased by increasing Gd^{3+} ions molar ratios. The saturation magnetization was found to be increased from 1.61 $A.m^2/kg$ for pure LSM to to 28.61 $A.m^2/kg$ for 0.4 Gd^{3+} ion substituted LSM sample.

Keywords: Lanthanum strontium manganite, Nanopowders, Citrate precursor method, Crystal structure, Optical properties, Magnetic properties

Introduction

Introduction

Solid oxide fuel cells (SOFCs) are one of the promising fuel cells that offer very high efficiency with fuel flexibility and low contamination to environment [1], [2], [3], [4] [5]. However, conventional SOFCs typically operates at very high temperatures (800–1000 °C), which bring various degradation problems [6]. Subsequently, anode, cathode and electrolyte materials must be stable at such operation temperature. In this regards, because of its thermal stability and chemical compatibility, Sr-doped $LaMnO_3$ (lanthanum strontium manganite-LSM) attracts substantial interest as a promising cathode material for SOFCs. In nanosized crystals, this material presents high catalytic activity for oxygen reduction as well as thermal expansion coefficient similar to that of the solid electrolyte (yttria stabilized zirconia-YSZ) and high electrical conductivity [7-12]. Otherwise, LSM has limited application at reduced temperatures due to its low oxygen ion conductivity and high activation energy for oxygen dissociation [13]. Therefore, in order to improve the electrode performance at the temperature region of intermediate temperature solid oxide fuel cell (IT-SOFCs), one commonly used strategy is to add an ionically conducting second phase into the electronically conducting LSM

material to form composite cathode materials [14] [15]. Meanwhile, doping with lower-valence cations at A and/or B sites leads to emergence of defects (either vacancies or changes in the oxidation state of transition metals) that modify the oxygen adsorption–desorption properties and thus enhancing the electrode performance[16][17]. In particular, a variety of methods are available to prepare the nanosized LSMO perovskite materials such as co-precipitation [18-20], sol–gel [21], hydrothermal[22], ball milling[23], spray pyrolysis [24], pulse laser deposition [25], molecular beam epitaxy [26], magnetron sputtering [27], metal–organic decomposition [28], electrochemical deposition [29] and aerosol pyrolysis [30]. Among these methods, the solution combustion synthesis has steadily gained popularity because it can generate reproducibly high purity powders of controlled sizes and shapes in very short time using low cost chemicals and simple equipment. [31-32]. Remarkably, it is well known that several previous work concentration of Gd^{3+} doped ceria (GDC) as an interesting electrolyte materials due to high ionic conductivity than YSZ electrolyte. However, from the best of our knowledge, there is no previous reports concerning the change of the optical, electrical and magnetic properties of Gd^{3+} ion doped LSM as well as the effect of gadolinium ions concentration [33-35]. With this premise, the manipulation of Gd^{3+} ion content on the magnetic, optical and electrical properties of LSM nanopowders was studied in details. Meanwhile, the impact of Gd^{3+} ion on the crystal structure and microstructure was also investigated. Finally, such given properties were compared with pure $La_{0.5}Sr_{0.5}MnO_3$ phase.

2. Materials and Methods

2.1. Materials

All the chemicals utilized in the present work involved lanthanum nitrate hexahydrate $La(NO_3)_3.6H_2O$ (Fluka Analytical 61520), anhydrous strontium nitrate $Sr(NO_3)_2$ (Sigma-Aldrich 13914), manganese acetate tetrahydrate $C_4H_6MnO_4$ (AppliChem A2606,0500), gadolinium nitrate hexahydrate $Gd(NO_3)_3.6H_2O$ (Alfa Aesar) and pure citric acid $C_6H_8O_7$ (El-Nasar pharmaceutical chemical Co 3281119001)were of analytical grade. Moreover, deionized water was used in the whole work.

2.2. Procedure

Gadolinium substituted lanthanum strontium manganite (LSM) nanopowders have been synthesized through citrate precursor route. In this regards, 0.5-*x*$La(NO_3)_3.$**$6H_2O$ was** mixed well with suitable ratios of strontium nitrate and manganese acetate tetrahydrate in the aqueous solution. Then, *x*$Gd(NO_3)_3.6H_2O$ was added to the solution at molar ratio of La:Sr:Mn:Gd was 0.5-*x*:0.5:1:*x* with various *x* values from 0.0 to 0.4. After that, certain amount of citric acid related to the metal salts was inserted to aqueous solutions to chelate with the metals ions. The citric acid was not only employed to form stable complexes also but also it was anticipated as an organic rich fuel. The solutions were slowly evaporated on a hot plate magnetic stirrer at 80°C to form viscous gel and then dried at 100°C for 24 h to contain the citrate precursors. Eventually, the dry precursors were heated at a rate of 10 °C/min in static air with different maximum holding temperatures ranging from 800 to 1200 °C where they were maintained for 2 h.

Table 1. Metal salts concentration used for preparation of $La_{1-x}Sr_xMnO_3$ nanopowders

Chemicals used	Pure LSM sample	Gd^{3+} ion content			
		0.1	0.2	0.3	0.4
$La(NO_3)_3.6H_2O$, mg	4.43	3.54	2.65	1.77	0.88
$Sr(NO_3)_2$, mg	2.11	2.11	2.11	2.11	2.11
$Gd(NO_3)_3.6H_2O$	-	0.90	1.80	2.70	3.61
$C_4H_6MnO_4.4H_2O$, mg	4.91	4.91	4.91	4.91	4.91
Citric acid , mg	16.81	16.81	16.81	16.81	16.81

2.3. Physical Characterization

X-ray powder diffraction (XRD) was executed on a model Bruker AXS diffractometer (D8-ADVANCE Germany) with Cu Kα (λ = 1.54056 Å) radiation, operating at 40 kV and 40 mA. The diffraction data were recorded for 2θ values between 10 and 80°. The morphologies of the formed powders were implemented by a Field emission scanning electron microscopy FE-SEM (JEOL-JSM-5410 Japan). The absorbance spectra were accomplished using UV-Vis-NIR-scanning spectrophotometer (JASCO V-570, Japan). Electrochemical impedance spectrums (EIS) were recorded as a function of frequency with 6 points with an AC perturbation signal of 50 mA using a PARSTAT 4000 Potentiostat/Galvanostat/EIS Analyzer. The magnetic properties of the formed materials were fulfilled using vibrating sample magnetometer (7400-1 VSM, lackshore, USA) in a maximum applied field of 20 kOe.

3. Results and discussion

3.1. Crystal structure

Fig.1 indicates the XRD profiles of Gd3+ ion substituted lanthanum strontium manganite synthesized by citrate precursor pathway annealed at 1000^{o}C for 2h. Plainly, diffraction peaks joined with pure monoclinic perovskite phase were coincided. For instance, peaks corresponded to JCPDS card (00-04900595) were indexed. Meanwhile, the space group of the produced powders was defined as P21/a for the diffraction peaks of the LSM with fully crystallized perovskite structure for all prepared samples. The average crystallite size of the Gd^{3+} substituted LSM particles was determined from the most intense peak of LSM based on Scherrer's formula.

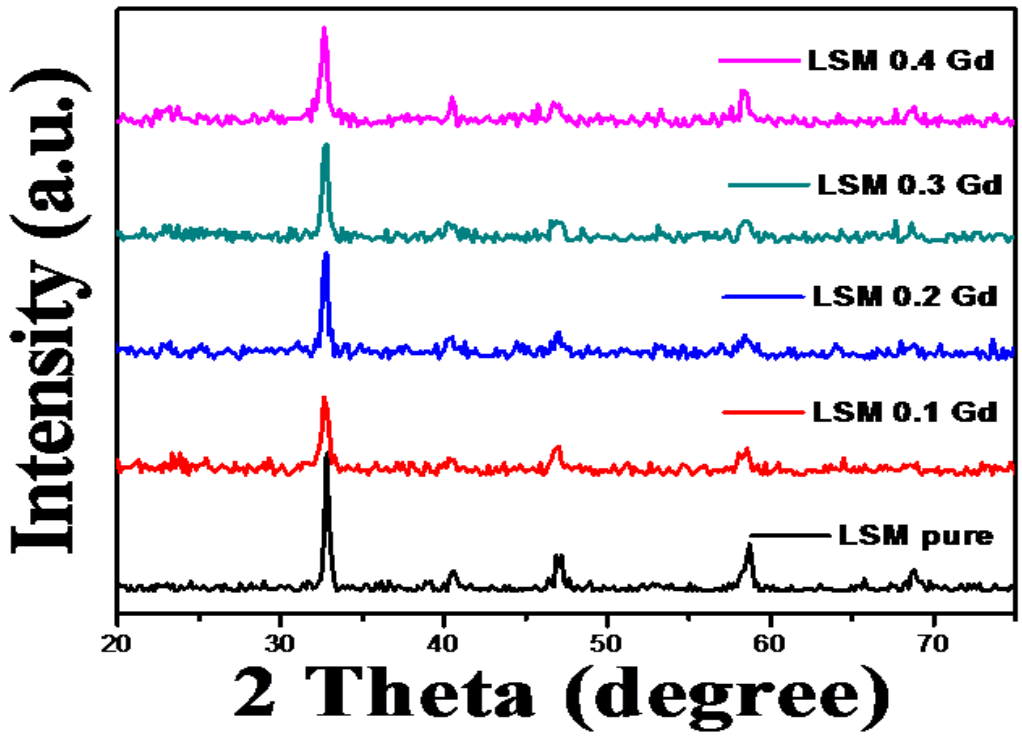

Fig.1: XRD patterns of produced pure and Gd^{3+} substituted LSM nanopowders by citrate precursors method at different Gd^{3+} ions molar ratios (0.1, 0.2, 0.3 and 0.4) annealed at 1000°C for 2 h.

The lattice parameters (*a, b, and c*) of LSM nanopowders can be obtained from the following equation:

$$\frac{1}{d^2} = \frac{1}{sin^2\beta}\left(\frac{h^2}{a^2} + \frac{k^2 sin^2\beta}{b^2} + \frac{l^2}{c^2} - \frac{2hl\ cos\beta}{ac}\right)$$

The unit cell volume *V* of the monoclinic system can be calculated by the following equation

$$V = abc \sin\beta$$

Where **a**, **b**, and **c** are the unit cell axes dimensions and **β**, is the inclination angle of the axe in the unit cell and (k,h,l) are called miller indices.

Table 1 records the change in crystallite size, lattice parameters and the unit cell volume of Gd3+ ion substituted LSM. Evidently, the crystallite size was found to first increase with Gd3+ molar ratio of 0.1 then it was decreased with further increased of Gd^{3+} ion content up to 0.4. The crystallite size was in the range between 25.6 to 35.1 nm. The variation of lattice parameters (*a,b* and *c*) was found to decrease with the extent of substitution of Gd^{3+} ion concentration. Subsequently, the unit cell volume was decreased. The results can be attributed to the small radius of Gd^{3+} ion (1.078 Å) compared to the radius of La^{3+} ion (1.36 Å) which follows that substitution of La^{3+} ion by Gd^{3+} ion can occur.

Table 1: Crystallite size, lattice constant and unit cell volume of Gd3+ ion substituted LSM synthesized using citrate precursor method annealed at 1000^{o}C for 2h

Gd^{+3} ion content	Crystallite size, nm	Lattice parameters, Å			Unit cell volume, $Å^3$
		a	***b***	***c***	
LSM	28.8	5.520	7.820	5.640	243.46
LSMG1	35.1	5.510	7.810	5.631	242.31
LSMG2	32.6	5.491	7.798	5.621	240.68
LSMG3	31.5	5.489	7.787	5.611	239.83
LSMG4	25.6	5.487	7.776	5.589	238.46

3.2. Microstructure

Fig. 2 (a, b, c and d)illustrates a representative field emission scanning electron micrographs (FE-SEM) of Gd^{3+} ions substituted LSM nanoparticles. The size variation of the particle attributed to the absence of any surfactant in the synthesis procedure. The formation of agglomerates was due to the annealing temperature. The loose and the porous structure of annealed samples can be attributed to significant gas evolution during combustion reaction.The transformation in the shape from monoclinic to spherical agglomerates was observed in the formed powders by increasing the Gd^{3+} ions content from 0.1 to 0.3. However at 0.4 Gd^{3+} ions molar ratios, the formed particles are connected to gather to form cluster with monoclinic shape.

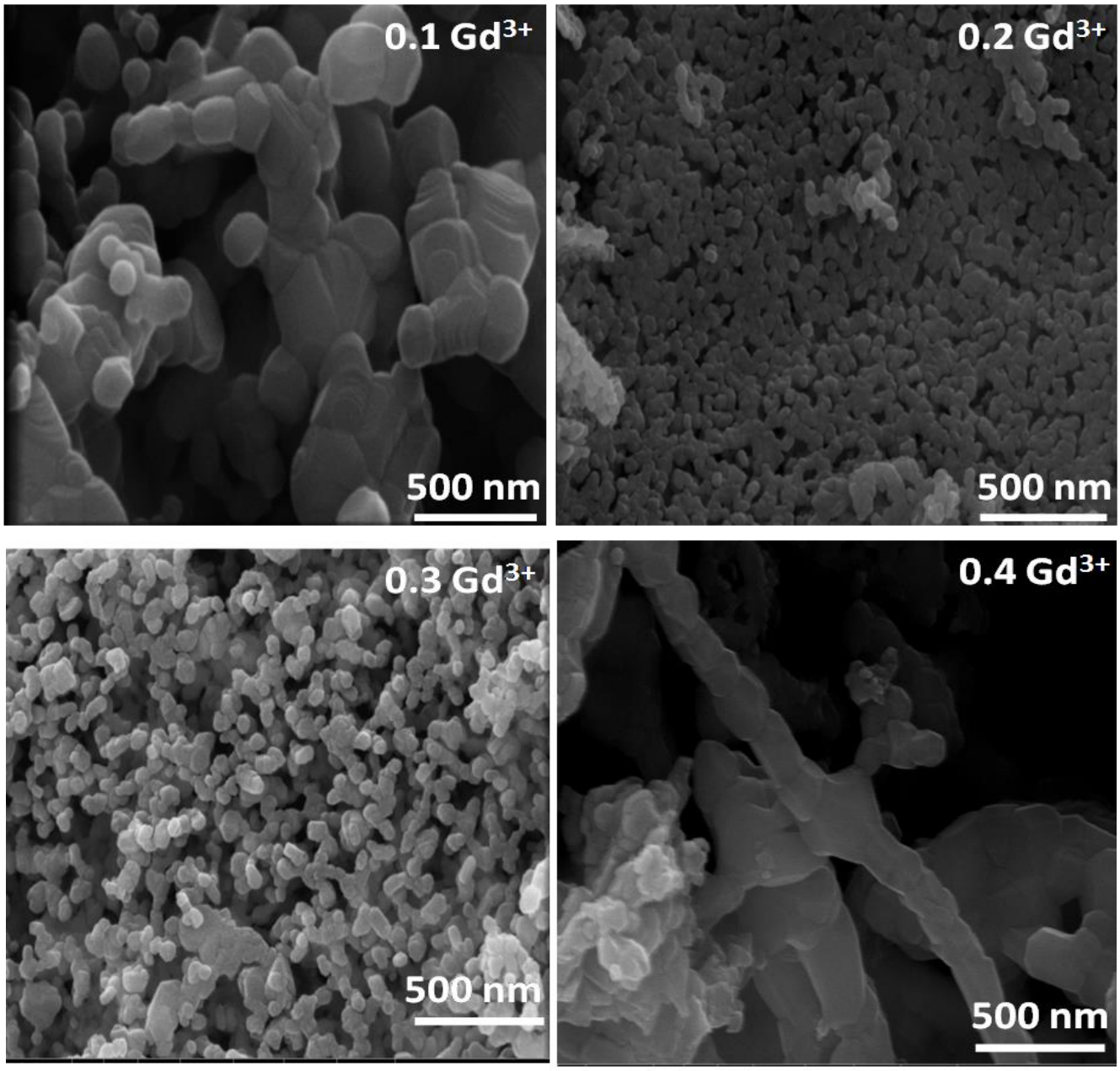

Fig.2: FE-SEM photograph of produced pure and doped Gd^{3+} substituted LSM nanopowders by citrate precursors method at different Gd^{3+} ions molar ratios: a) 0.1, b) 0.2, c) 0.3 and d) 0.4, annealed at 1000^{o}C for 2 h.

3.3. Optical properties

Fig. 3 displays the reflectance spectra of LSM measured in the wavelength range of 200–800 nm. It can be seen that the reflectance of the low Gd^{3+} ion concentration is slightly higher than that of unsubstituted LSM nanopowders. The maximum reflectance was ~40 % for the powders synthesized at 0.4 Gd^{3+}ion content. The wavelength was around 280 nm for substituted sample and 260 for un substituted sample respectively. Fig.4 indicates the absorbance spectra of pure LSM and Gd^{3+} ions doped lanthanum strontium manganite. The increasing of gadolinium ions molar ratios enhances the optical absorbance of produced nanopowders. In addition, a small increasing of the edge of the absorbance spectra at the wavelengths from 200-800 nm is observed. The band gap energy of the formed LSM substituted with gadolinium ions are presented in Fig. 5. It shows that the band gap energy was decreased with increasing the gadolinium ions substitution. It was decreased from 2.45 eV at LSM pure sample to 2.39 eV at 0.1 Gd^{3+} then to 2.19 eV at 0.2 Gd^{3+}.The band gap energy was decreased to be 1.75 eV at 0.3 $Gd^{3+}$and 1.63 eV at 0.4 Gd^{3+} ions content. This can indicate the presence of intermediate energy levels within the band gap between valence band and conduction band. The intermediate energy levels or localized state related to the ordered – disordered structure. The ordered structure of LSM powders can be explained as (MnO_6)-(MnO_{6-x}) clusters, which their cation and vacancy at the A- or B- site arranged in order that gives rise to perfect lattice crystalline. The (MnO_6)-(MnO_{6-x}) clusters are only relevant when any other defects are not presented, e.g. A- or B-site metal vacancies, while a disordered structure suggests the representative metal randomly distributed in pervoskite structure[37-38].

The energy-dependent transmittance spectra of LSM nanopowders prepared by citrate precursor method at calcination temperature of 1000 ^{o}C for 2 h with different metal ion

substitutions are obtained experimentally and presented in Fig. 6.The addition of Gd^{3+} ions into La^{3+}ions depended on the ionic size and electronegativity difference between the two metal ions. Since the A site ions in ABO_3 structure are fully ionized, the electronegativity difference is of minor importance although local structural distortions may be sensitive to local ionic radii and their variations. Finally, possible effects due to integral charge states (Mn^{3+}, Mn^{4+}) will be averaged in E_g calculations in the highly conducting regime where our treatment will be most realistic. The actuations between the transmittance spectra of LSM substituted gadolinium at different concentrations varying from (0.1to 0.4). Hence, cut of around 1.6 eV was observed which arises due to the transitions from the oxygen states at the uppermost valence band to Gd^{3+} states at the lowermost conduction band. The rising trend of the experimental data for both LSM at the higher-energy side may show a tendency to give another absorption peak corresponding to the electronic transition from the semi-core states in the valence band to conduction band [39].

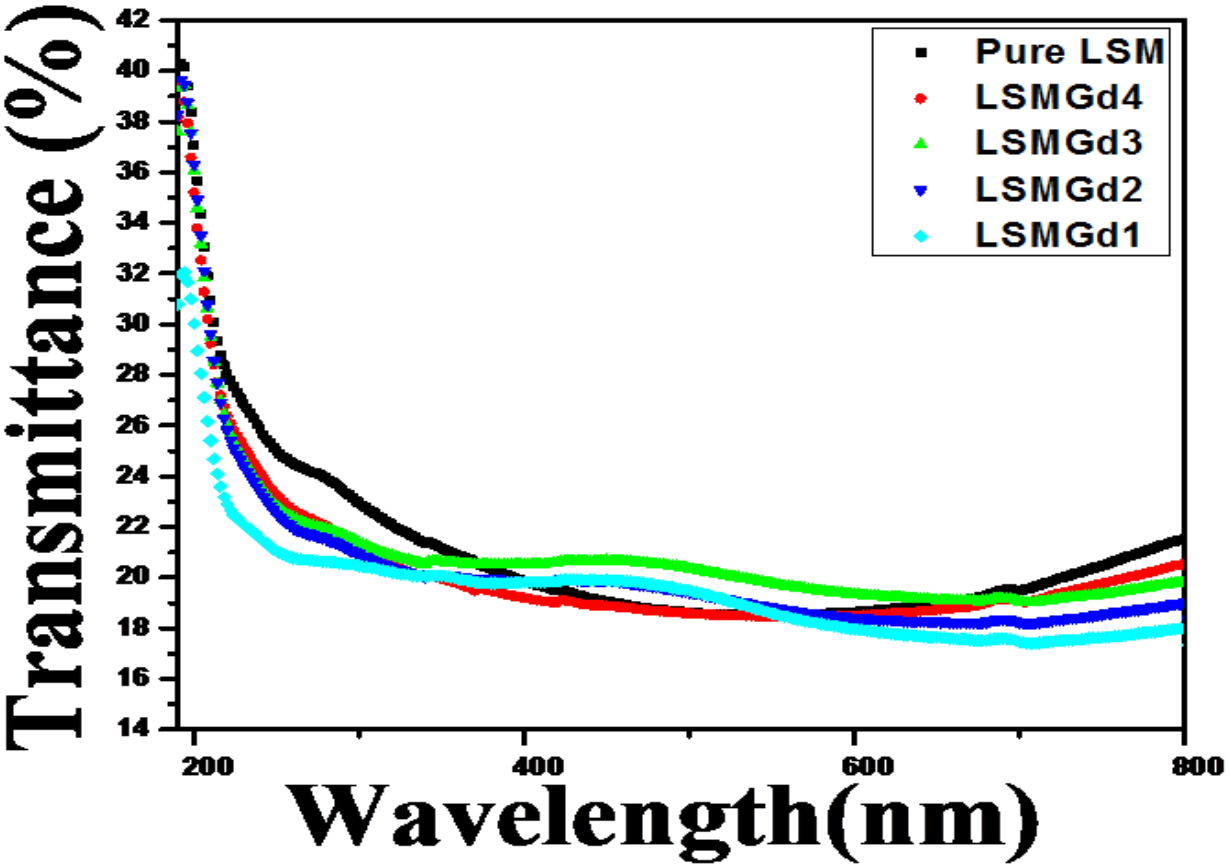

Fig. 3: Reflectance spectra of LSM nanopowders synthesized by citrate method at calcination temperature of 1000 ^{o}C with different Gd^{3+} ions concentrations (0, 0.1, 0.2, 0.3 and 0.4)

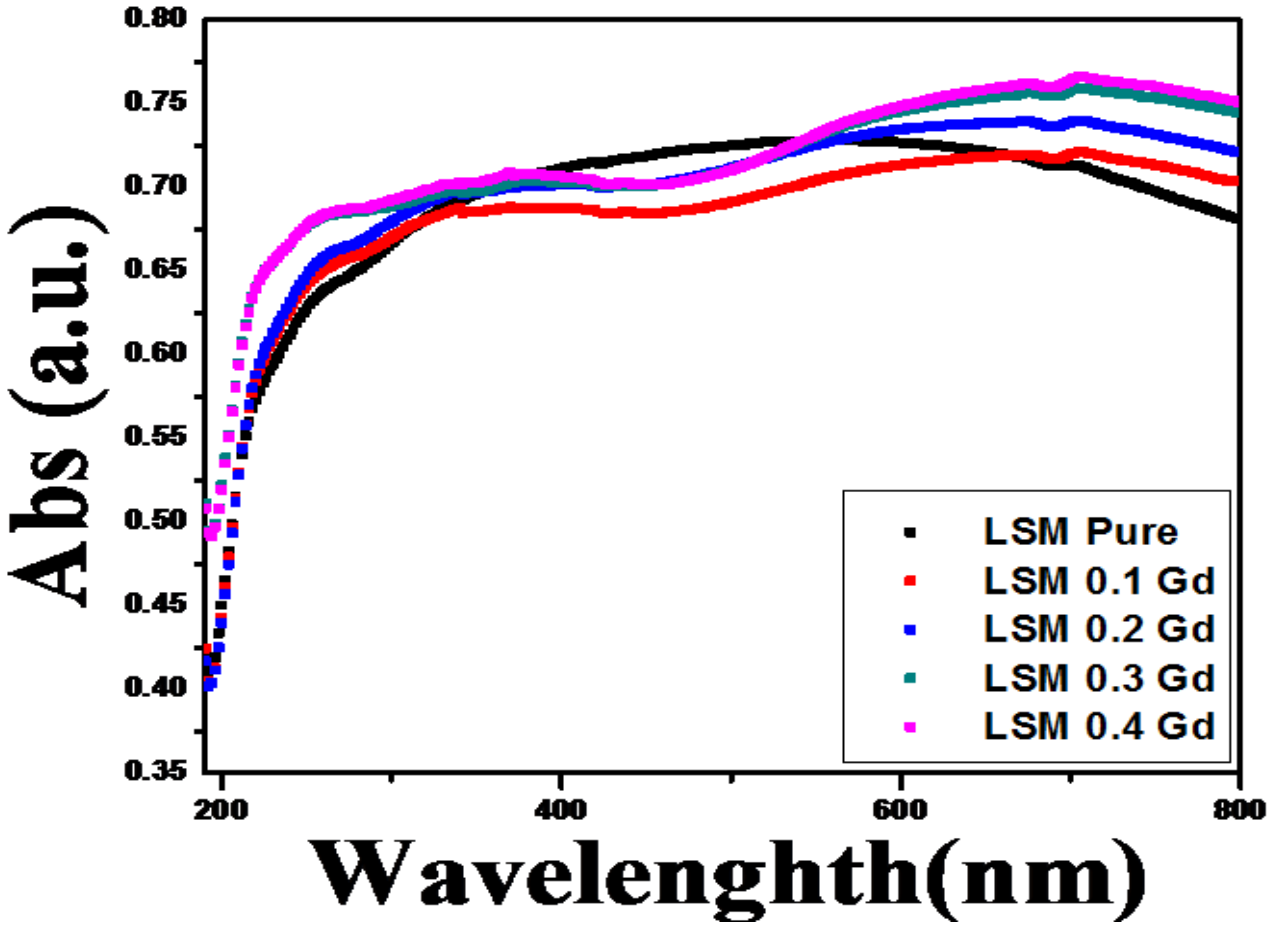

Figure 4. Absorbance spectrum of LSM nanopowders synthesized using citrate method at calcination temperature of 1000 ^{o}C with different Gd^{3+} ions contents (0, 0.1, 0.2, 0.3, and 0.4).

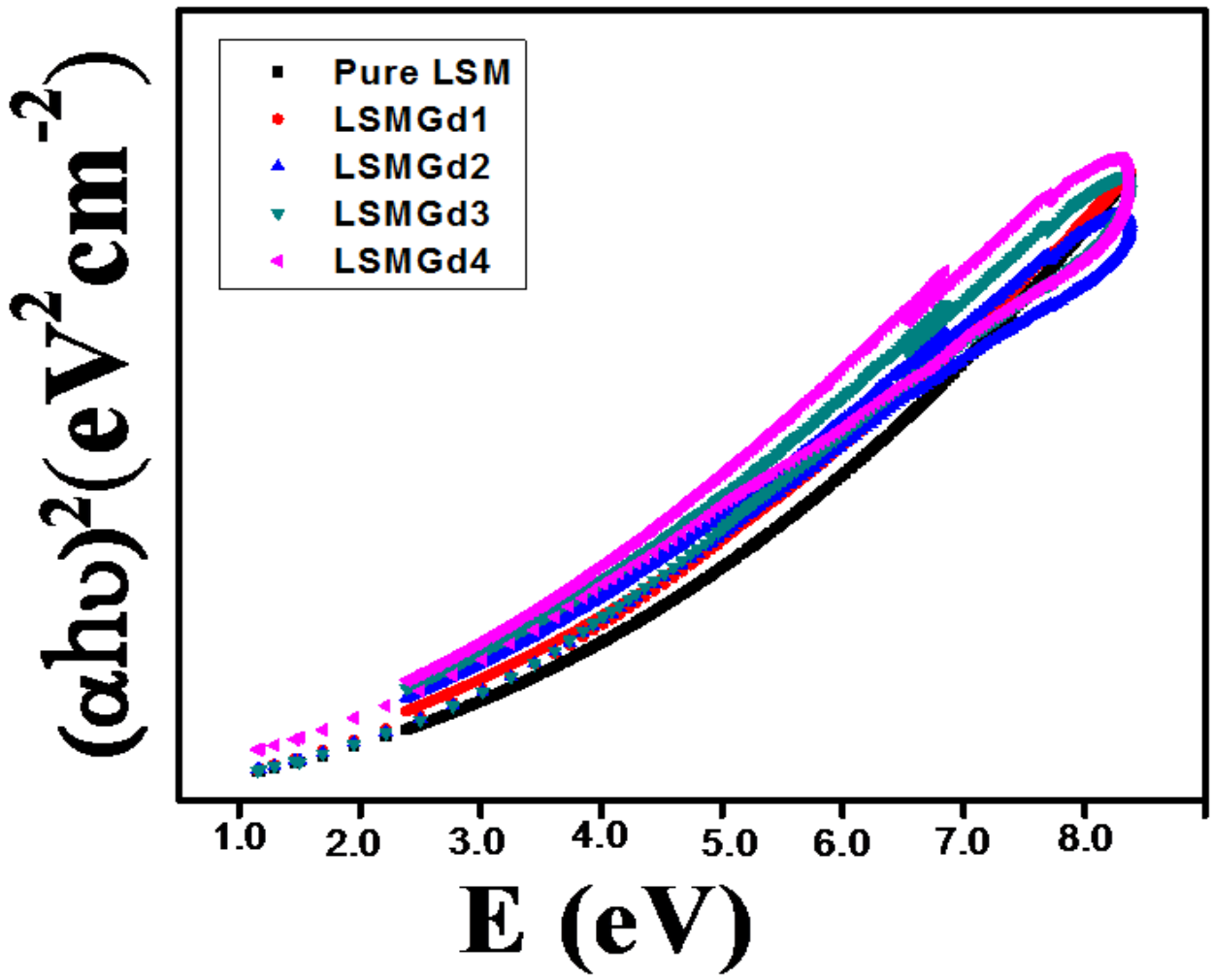

Figure 5. The band gap energy of LSM nanopowders at different Gd^{+3} ion contents (0, 0.1, 0.2, 0.3 and 0.4)

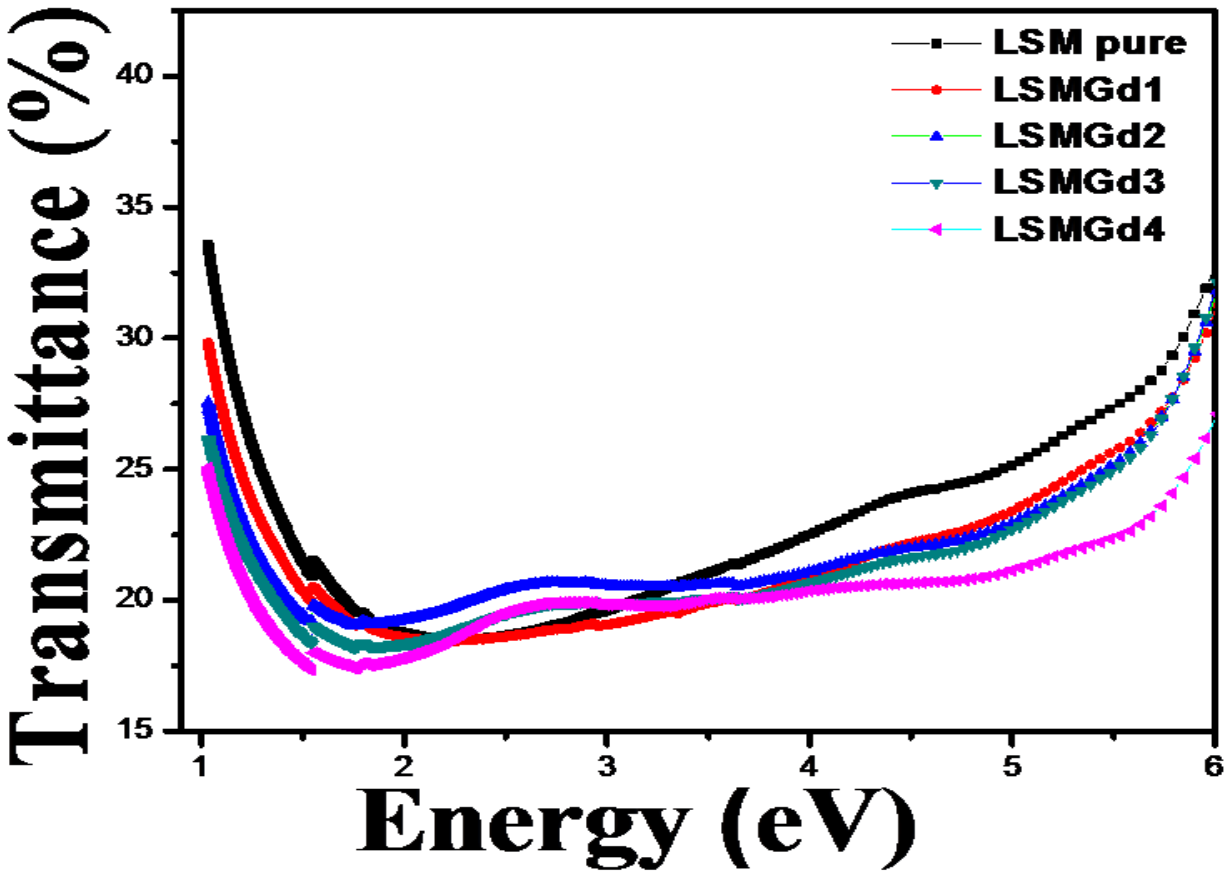

Fig. 6: Transmittance spectra as a function of photon energy for LSM nanopowders prepared via citrate method annealed at 1000 ^{o}C for 2h with different Gd^{3+} ions molar ratios (0, 0.1, 0.2, 0.3 and 0.4).

3.4. Electrochemical impedance spectroscopy

Fig. 7 presents the impedance spectra of the lanthanum strontium manganite cathode substituted by gadolinium ions and prepared via citrate precursor method at calcinations temperature of 1000 °C for 2 h. As can be seen, they are composed of large depressed arcs located in between the high frequency and the low frequency zones, respectively. The Nyquist plots have been fitted using an equivalent circuit constituted of an inductance *L*, a resistance*R*1 and two constant phase elements (CPE1 and CPE2) in parallel with resistor (*R*2 and*R*3), as shown inFig.8. In this equivalent circuit, R1 corresponds to the electrolyte resistance, electrode ohmic resistance and lead resistance.*R*2 represents the polarization resistance associated with the high frequency charge transfer process and*R*3 represents that associated with low frequency oxygen adsorption and dissociation processes [40-41]. It can be seen that both the ohmic resistance (*R*s) and polarization resistance (*R*p) of the electrode were increased by increasing Gd^{3+} ions concentration. Otherwise both the ohmic resistance (*R*s) and polarization resistance in the doped samples were higher than the pure LSM sample. The smaller arc at both high frequency and low frequency can be attributed to faster charge transfer process, higher specific surface area of the cathode, faster oxygen dissociation and surface diffusion processes.

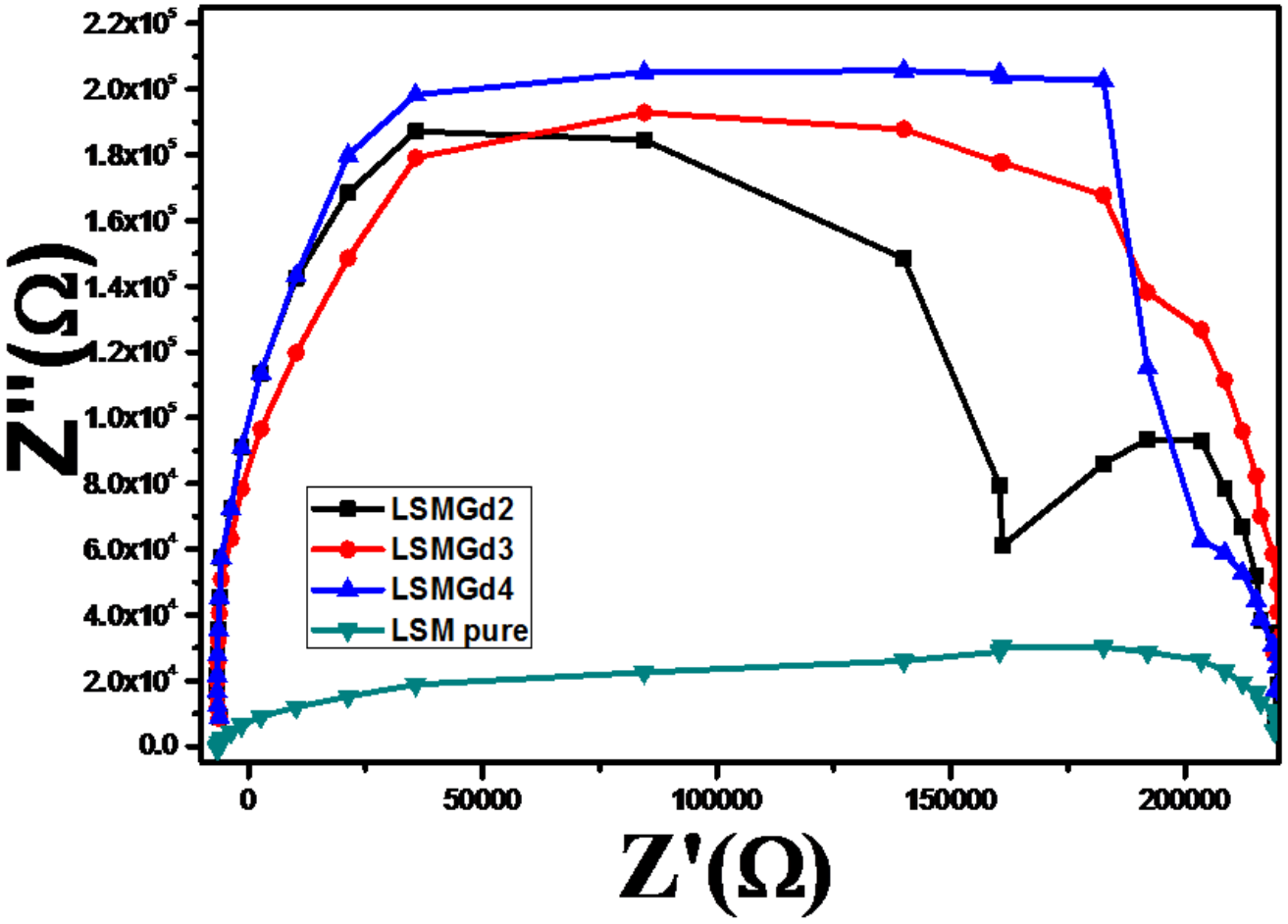

Figure 7. The Nequest diagram of LSM nanopowders at different Gd^{+3} ion content (0.1, 0.2, 0.3 and 0.4)

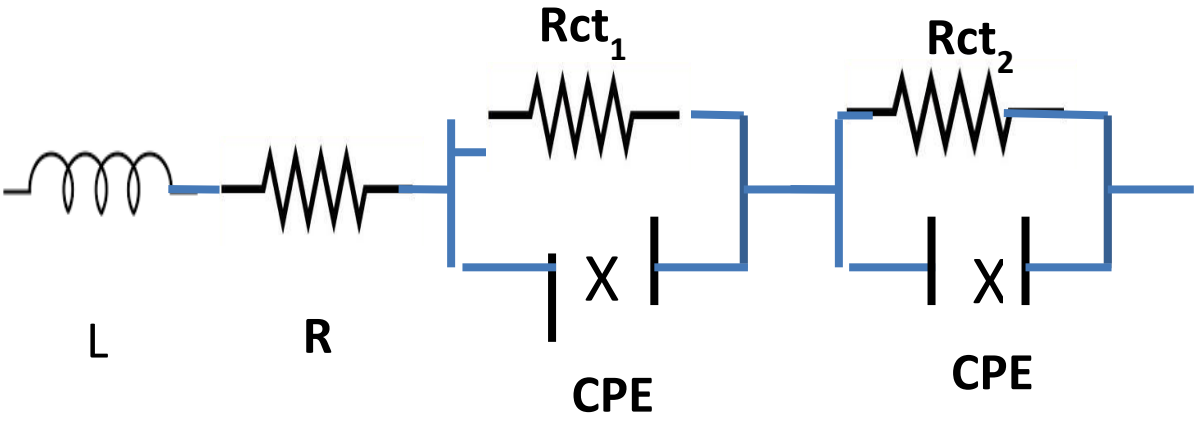

Figure 8. The equivalent circuit schematic diagram of $La_{0.5-x}Sr_{0.5}Gd_x MnO_3$powders

3.5. Magnetic properties

Fig. 9 depicts the magnetic properties of Gd^{3+} ion substituted LSM synthesized using citrate precursor strategy annealed at 1000^{o}C for 2h. Furthermore, the change in the magnetic parameters is summarized in Table 2. Evidently, it is demonstrated that the value of magnetization was found to increase with the applied magnetic field and it did not attain saturation due to the smallest average crystallite size of the produced powders. These nanosized particles are much smaller than the magnetic domain. Accordingly, the saturation does not achieve the degree of magnetic saturation and the corresponding magnetization values were strongly dependent on the composition of the produced materials. The increase in magnetization for Gd^{3+} substitution might be due to replacement of La with no magnetic moment μ_{eff}= 0 μ_B by effective magnetic moment μ_{eff}=8 μ_B, resulting in an increase in the magnetic moment of the magnetic ions. Furthermore, the A–O bond size was enhanced where the smaller Gd^{3+} ions replace the larger La^{3+} ions. By increasing the Gd^{3+} ions content, the unit cell volume is slightly decreased which is expected result imputed to to the small difference between the two ionic radii. Furthermore, the increase of magnetizartion with the increase of Gd^{3+}content is attributed to the higher density of the unpaired electron ($4f^7$) compared with ($4f^0$) of La^{3+} ion in the produced samples which deals with previous published elsewhere [42]

The change of coercivity with the increase of the Gd^{3+}amount in doped lanthanum strontium manganite is illustrated in Table 3. The coercivity was found to increase as the amount of gadolinium substitution increased. This result was obtained previously in other kind of materials [43]and it can be explained as follows: Gd^{3+} and Mn^{2+} ions have stronger coupling and weaker crystal field, so they have stronger magneto crystalline anisotropy [44]. The intrinsic magnetic nature of Gd^{3+} ion plays an important role in the overall magnetic behavior

of the system. Due to the ionic radii mismatch of Gd^{3+} and Sr^{2+}, it is interesting to study the effect of gadolinium ions doping on the magnetism in $La_{0.5-x}Sr_{0.5}Gd_xMnO_3$ system. The symmetry of crystal will be decreased after the sample was substituted by Gd^{3+} ions. Hence there is a distortion in lattice field which generates an internal stress (Table1). Furthermore, the crystallite size decreases as the amount of Gd^{3+} increases(Table 1), hence the grain boundary increases. So, the area of disordered arrangement for ions on grain boundaries may fix and hinder the domain walls motion, thus the coercivity of the samples increases with Gd^{3+}substitution ions. Moreover, when Gd^{3+}ion is added to any system, the magnetic behavior (as coercive field) of the system can increase. The results were in agreement with the previous published result by Shlapa *et al.* [45]. However, the saturation magnetization was particle size dependent. It was found that the saturation magnetization was increased with increasing the particle size as the further increasing of Gd^{3+} ion content. For instance, the surface magnetic anisotropy originating from a magnetically disordered surface layer known as a dead or passivating layer existed in the nanoparticles is usually the evidence of the phenomenon. With decreasing particle sizes, the thickness of the passivating layer and the number of disordered spins increases, which are adverse to the ferromagnetic order, thus leading to the reduction of magnetization and the increase of coercivity (*Hc*)and the magnetic retentivity (*Mr*) [37]. In comparison, Joy*et al.* measured the magnetic hysteresis loops for $Gd_{1-x}Sr_xMnO_3$(x=0.3, 0.5, 0.6) thin films up to 70 kOe at 10 and 300 K. They found that the coercivity of thin films is lower than that of bulk. This is due to the lower crystallinity and smaller grain size of thin films [46].

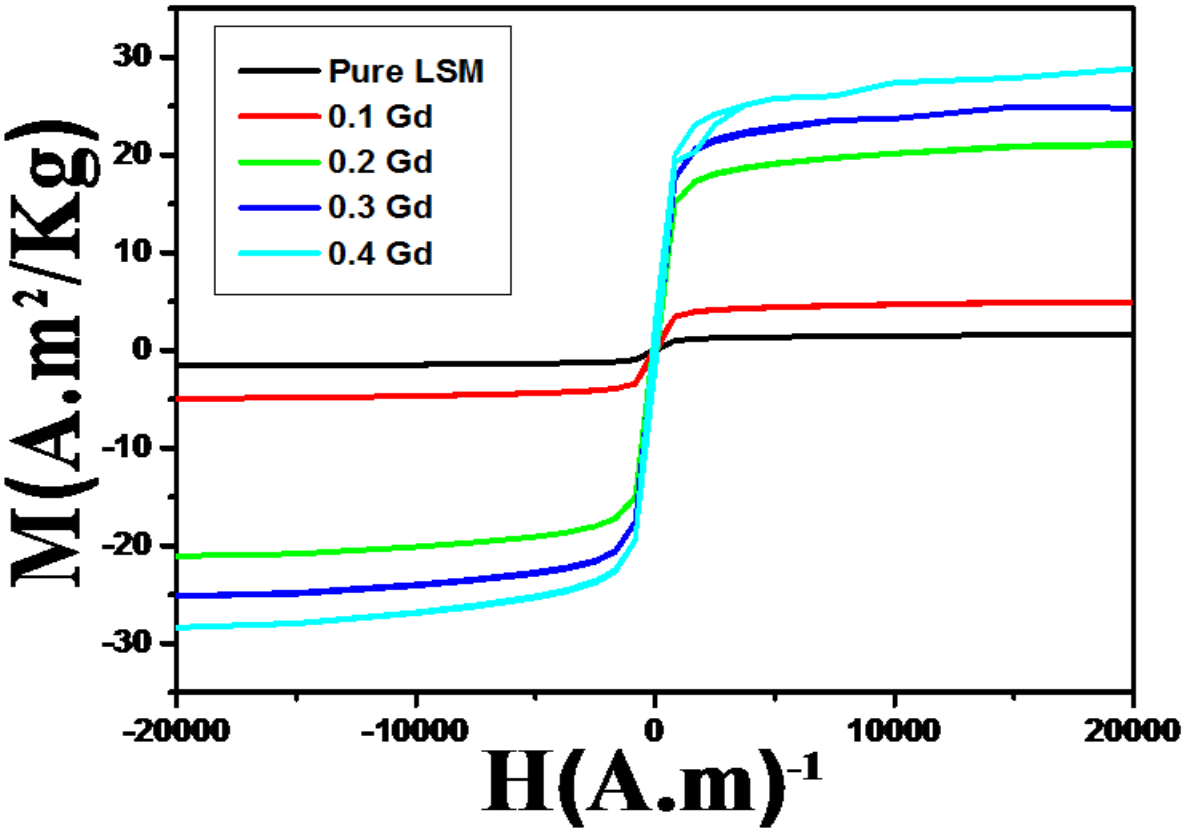

Figure 9: M-H hysteresis curves of ($La_{0.5-x}Sr_{0.5}Gd_xMnO_3$) synthesized by organic acid precursor annealed at 1000 ºC for 2 h at different Gd^{+3} ion molar ratios (0, 0.1,0.2, 0.3 and 0.4)

Table 2: Magnetic properties of Gd^{3+} ion substituted LSM powders synthesized using citrate precursor method annealed at 1000°C for 2h

Sample ID	**Magnetic properties**		
	***Ms*, A.m^2/kg**	***Mr*, A.m^2/kg**	***Hc*, (A.m)$^{-1}$**
LSM pure	1.607	0.068	54.43
0.1 Gd^{3+}	4.940	0.376	81.90
0.2Gd^{3+}	21.106	2.000	97.50
0.3Gd^{3+}	25.194	1.381	60.48
0.4 Gd^{3+}	28.612	2.378	90.52

3.6. Conclusion

Gadolinium doped lanthanum strontium manganite (GLSM) nanopowders $La_{0.5-x}Sr_{0.5}Gd_xMnO_3$ ($0.0 \leq x \leq 0.4$) were systematically prepared using citrate-precursor method. Indeed, the samples were annealed at temperature 1000°C for time 2h to contain pure monoclinic GLSM phase. Evidently, the average crystallite size of the formed powders was in the range between 25 to 35 nm. The microstructure of the formed materials was substantially premised on the Gd^{3+} ion content. Clearly, the morphology was transformed from monoclinic like structure to spherical agglomerates by increasing the addition of Gd^{3+} ions from 0.1 to 0.3. Otherwise, the formed particles were exhibited clusters with continuously increased the Gd3+ ratio to 0.4. The band gap energy of the produced GLSM powders was decreased by increasing the Gd3+ ion content. Evidently, it was decreased from 2.45 to 1.63 eV with increasing the Gd3+ ion concentration from 0.0 to 0.4. Furthermore, the polarization resistance in the Gd^{3+} doped samples was higher than the pure LSM sample. The smaller arc at both high frequency and low frequency can be attributed to faster charge transfer process. Meanwhile, the saturation magnetization was found

to increase with increasing the Gd^{3+} ion. Indeed, the saturation magnetization (*Ms*) was increased from 1.61 $A.m^2/kg$ for pure LSM to 28.6 $A.m^2/kg$ with Gd^{3+} ion molar ratio of 0.4. Overall, the obtained nanopowders could be interested in several applications such as electrodes for potentiometric oxygen sensor and resistive switching devices. Moreover, Such properties would promise them for the effort candidate for biomedical applications

References

[1] S.P. Jiang, Development of lanthanum strontium manganite perovskite cathode materials of solid oxide fuel cells: a review J. Mater. Sci. 2008, 43, 6799-6833.

[2] S.D. Park, J.M. Vohs, R.J. Grote, Direct oxidation of hydrocarbons in a solid-oxide fuel cell, Nature ,2000, 404, 265-267.

[3] L. Yang, C.D. Zuo, S.Z. Wang, K. Blinn, M.F. Liu, Z. Cheng, M.L. Liu, Enhanced sulfur and coking tolerance of a mixed ion conductor for SOFCs: $BaZr_{0..1}Ce_{0.7}Y0._{2-x}Yb_xO_{3-\delta}$, Science 2009, 326 126 -129.

[4] Z.L. Zhan, S.A. Barnett, An octane-fueled solid oxide fuel cell, Science, 2005, 308,844-847.

[5] C.C. Wang, L.H. Luo, Y.F. Wu, B.X. Hou, L.L. Sun, A novel multilayer aqueous tape casting method for anode-supported planar solid oxide fuel cell, Mater. Lett.2011, 65, 2251-2253.

[6] D.J.L. Brett, A. Atkinson, N.P. Brandon, S.J. Skinner, Intermediate temperature solid oxide fuel cells, Chem. Soc. Rev. ,2008,37, 1568-1578

[7] da Concei¸c˜ao Leandro, Silva Camila R.B., Ribeiro Nielson F.P., Souza Mariana M.V.M., Influence of the synthesis method on the porosity, microstructure and electrical properties of $La_{0.7}Sr_{0.3}MnO_3$ cathode materials, Materials Characterization , 2009,60, 1417-1423

[8] M. Asamoto, H. Yamaura, H. Yahiro, Influence of microstructure of perovskite-type oxide cathodes on electrochemical performances of proton-conducting solid oxide fuel cells operated at low temperature, J. Power Sources ,2011,196, 1136-1140.

[9] G.S. Godoi, D.P.F. de Souza, Electrical and microstructural characterization of $La_{0.7}Sr_{0.3}MnO_3$ (LSM), $Ce_{0.8}Y_{0.2}O_2$ (CY) and LSM–CY composites,Mater. Sci. Eng. B 2007,140, 90-97.

[10] M.Z. Li Lv, Z.T. Wei, X.S. Yang, X. Zhang, Transport properties and microstructure of $La_{0.7}Sr_{0.3}MnO_3$ nanocrystalline thin films grown by polymer-assisted chemical solution deposition, J. Mod. Transp. ,2014, 22 50-54.

[11] H. Jalili, J.W. Han, Y. Kuru, Z.H. Cai, B. Yildiz, New insights into the strain coupling to surface chemistry, electronic structure, and reactivity of $La_{0.7}Sr_{0.3}MnO_3$, J. Phys. Chem. Lett. , 2011, 2, 801-807.

[12] K. Chen, Z. Lü, X.J. Chen, N. Ai, X.Q. Huang, X.B. Du, W.H. Su, Development of LSM-based cathodes for solid oxide fuel cells based on YSZ films, J. Power Sources ,2007,172, 742-748.

[13] X.Y. Xu, C.R. Xia, G.L. Xiao, D.K. Peng, Fabrication and performance of functionally graded cathodes for IT-SOFCs based on doped ceria electrolytes ,Solid State Ionics, 2005, 176, 1513-1520.

[14] X. Xu, Z. Jiang, X. Fan, C. Xia, LSM–SDC electrodes fabricated with an ion-impregnating process for SOFCs with doped ceria electrolytes, Solid State Ionics, 2006 177,2113-2117.

[15] V.A.C. Haanappel, J. Mertens, D. Rutenbeck, C. Tropartz, W. Herzhof, D. Sebold, F. Tietz, Optimisation of processing and microstructural parameters of LSM cathodes to improve the electrochemical performance of anode-supported SOFCs, J. Power Sources, 2005 141, 216-226.

[16] G. Saracco, F. Geobaldo, G. Baldi, Methane combustion on Mg-doped $LaMnO_3$ perovskite catalysts, Appl. Catal. B Environ. , 1999, 20, 277-288.

[17] K.K. Hansen, K. Vels Hansen, A-site deficient $(La_{0.6}Sr_{0.4})_{1-s}Fe_{0.8}Co_{0.2}O_{3-\delta}$ perovskites as SOFC cathodes,Solid State Ionics ,2007, 178 , 1379-1384.

[18] Lu Gan, Qin Zhong, Xiaolu Zhao, Yang Song, Yunfei Bu, Structural and electrochemical properties of B-site Mg-doped $La_{0.7}Sr_{0.3}MnO_{3-\delta}$ perovskite cathodes for intermediate temperature solid oxide fuel cells, Journal of Alloys and Compounds ,2016, 655, 99-105

[19] Z.F. Zi, Y.P. Sun, X.B. Zhu, Z.R. Yang, J.M. Dai, W.H. Song, Synthesis of magnetoresistive $La_{0.7}$ $Sr_{0.3}$ MnO_3 nanoparticles by an improved chemical coprecipitation method, J. Magn. Magn. Matter, 2009, 321, 2378–2381.

[20] Y. Luo, I. Szafraniak, N.D. Zakharov, V. Nagarajan, M. Steinhart, R.B. Wehrspohna, J.H. Wendorff, R. Ramesh, M. Alexe, Nanoshell tubes of ferroelectric lead zirconate titanate and barium titanate, Appl. Phys. Lett. ,2003, 83, 440.

[21] Z.F. Zi, Y.P. Sun, X.B. Zhu, C.Y. Hao, X. Luo, Z.R. Yang, J.M. Dai, W.H. Song, Electrical transport and magnetic properties in $La_{0.7}$ $Sr_{0.3}$ MnO_3 and $SrFe_{12}O_{19}$ composite system, J. Alloys Compd. ,2009, 477, 414.

[22] A. Rostamnejadi, H. Salamati, P. Kameli, H. Ahmadvand, Superparamagnetic behavior of $La_{0.67}$ $Sr_{0.33}$ MnO_3 nanoparticles prepared via sol–gel method, J. Magn. Magn.Matter , 2009, 321, 3126.

[23] T.-Y. Chen, K.-Z. Fung, Synthesis of and densification of oxygen-conducting $La_{0.8}Sr_{0.2}Ga_{0.8}Mg_{0.2}O_{2.8}$ nano powder prepared from a low temperature hydrothermal urea precipitation process, J. Eur. Ceram. Soc. , 2008, 28, 803.

[24] P. Kameli, H. Salamati, A. Aezami, Influence of grain size on magnetic and transport properties of polycrystalline $La_{0.8}$ $Sr_{0.2}$ MnO_3 manganites, J. Alloys Compd. ,2008, 450, 7-11.

[25] A. Abrutis, A. Teiserskis, G. Garcia, V. Kubilius, Z. Saltyte, Z. Salciunas, V. Faucheux, A. Figueras, S. Rushworth, Preparation of dense, ultra-thin MIEC ceramic membranes by atmospheric spray-pyrolysis technique, J. Membr. Sci. ,2004, 240, 113-122.

[26] T.R. McGuire, A. Gupta, R.P. Duncombe, M. Rupp, J.Z. Sun, R.B. Laibowitz, W.J. Gallager, X. Gang, Magnetoresistance and magnetic properties of $La_{1-x}Sr_xMnO_{3-\delta}$ thin films, J. Appl. Phys., 1996, 79 , 45-49.

[27] E.S. Vlakhov, R.A. Chakalov, R.I. Chakalov, K.A. Nenkov, K. Dorr, A. Handstein, K.H. Muller, Influence of the substrate on growth and magnetoresistance of $La_{0.7}Ca_{0.3}MnO_z$ thin films deposited by magnetron sputtering, J. Appl. Phys ,1998, 83 , ,2152.

[28] Z. Yang, L. Sun, C. Ke, X. Chen, W. Zhu, O. Tan, Growth and structure properties of $La_{1-x}Sr_xMnO_{3-\sigma}$ (x= 0.2, 0.3, 0.45) thin film grown on $SrTiO_3$ (001) single-crystal substrate by laser molecular beam epitaxy, J. Cryst. Growth , 2009, 311, 3289.

[29] X. Zhu, H. Shen, Z. Tang, K. Tsukamoto, T. Yanagisawa, M. Okutomi, N. Higuchi, Structural and magnetotransport properties of $La_{0.67}Sr_{0.33}MnO_z$ thin films prepared by metal–organic decomposition under different annealing process, J. Alloys Compd. 488, 2009, 437.

[30] A. Gedanken, Preparation of $La_{1-x}Sr_xMnO_3$ nanoparticles by sonication-assisted coprecipitation, Mater. Res. Bull. , 2003, 38, 11.

[31] H.B Wang, J.F. Gao, D.K. Peng, G.Y. Meng, Plasma deposition of $La_{0.8}Sr_{0.2}MnO_3$ thin films on yttria-stabilized zirconia from aerosol precursor, Mater. Chem. Phys. ,2001, 72 297.

[32] Chuan Wang, Xianshuang Xin, Yanjie Xu, Jianyin Chen, Le Shao, Juan Zhou, Shaorong Wang, Tinglian Wen , Easy sintering of silver doped lanthanum strontium manganite current collector for solid oxide fuel cells, International Journal of Hydrogen Energy, 2011, 36 , 7683–7687

[33] M. Balaguer, V.B. Vert, L. Navarrete, J.M. Serra, SOFC composite cathodes based on LSM and co-doped cerias ($Ce_{0.8}Gd_{0.1}X_{0.1}O_{2-\delta}$, X= Gd, Cr, Mg, Bi, Ce), Journal of Power Sources, 2013, 223 , 214-220.

[34] Sun Jae Kim, Sun Woong Kim, Young Min Park, Kun Joong Kim, Gyeong Man Choi, Effect of Gd-doped ceria interlayer on the stability of solid oxide electrolysis cell, Solid State Ionics, 2016, 295, 25-31

[35] Clément Nicollet, Aurélien Flura, Vaibhav Vibhu, Aline Rougier, Jean-Marc Bassat, Jean-Claude Grenier, An innovative efficient oxygen electrode for SOFC: Pr_6O_{11} infiltrated into Gd-doped ceria backbone, International Journal of Hydrogen Energy, 2016, 41 , 15538-15544.

[36]M.M. Savosta, V.N. Krivoruchko, I.A. Danilenko, V.Y. Tarenkov, T.E. Konstantinova, A. V. Borodin,et al. Nuclear spin dynamics and magnetic structure of nanosized particles of $La_{0.7}Sr_{0.3}MnO_3$, Phys Rev B, 69 (2004), p. 024413

[37] A.S. Mazur, V.N. Krivoruchko, I.A. DanilenkoPhase separation in nanoscale samples of (LaSr)MnO_3, Low Temp Phys, 33 (2007), pp. 931-934

[38]IgorDanilenkoTetyanaKonstantinovaGalinaVolkovaValentinaGlazunova,$La_{0.7}Sr_{0.3}MnO_3$ nanopowders: Synthesis of different powders structures and real magnetic properties of nanomanganites, Materials Characterization, Volume 82, August 2013, Pages 140-145

[39] Gang Chen ,Yu Gao, Yifei Luo ,RuifengGuoaEffect of A site deficiency of LSM cathode on the electrochemical performance of SOFCs with stabilized zirconia electrolyte Ceramics International , 2017, 43, 1304–1309

[40] AO Turky, MM Rashad, AM Hassan, EM Elnaggar, M Bechelany, Tailoring optical, magnetic and electric behavior of lanthanum strontium manganite $La_{1-x}Sr_xMnO_3$ (LSM) nanopowders prepared via a co-precipitation method with different Sr2+ ion contents
RSC Advances, 2016, 6, 17980-17986

[41] A.O. Turky, M.M Rashad, A.T. Kandil, M. Bechelany, Tuning the optical, electrical and magnetic properties of $Ba_{0.5}Sr_{0.5}Ti_xM_{1-x}O_3$ (BST) nanopowders, Physical Chemistry Chemical Physics , 2015, 17 , 12553-12560

[42] M.M. Rashad, S. M. ElSheikh, Mater. Res. Bull. 46(3), (2011) 469

[43] A.O. Turky, M.M Rashad, AM Hassan, EM Elnaggar, M Bechelany , Optical, electrical and magnetic properties of lanthanum strontium manganite $La_{1-x}Sr_xMnO_3$ synthesized through the citrate combustion method, Physical Chemistry Chemical Physics, 2017, 19, 6878-6886

[44] Zein K. Heib, Mohamed Bakr Mohamed, L. Arda, N. Dogan, Cation distribution correlated with magnetic properties of nanocrystalline gadolinium, substituted nickel ferrite, Journal of Magnetism and Magnetic Materials, , 2015, 391, 195–202

[45] YuliaShlapa, SergiiSolopan, AndriiBodnaruk, MykolaKulyk, Viktor Kalita, YuliaTykhonenko-Polishchuk, AlexandrTovstolytkin, Victor Zinchenko, AnatoliiBelous, Lanthanum-strontium manganites for magnetic nanohyperthermia: Fine tuning of parameters by substitutions in lanthanum sublattice
Journal of Alloys and Compounds, 2017, 702, 31–37

[46] ZK Heiba, MB Mohamed, L Arda, N Dogan , Cation distribution correlated with magnetic properties of nanocrystalline gadolinium substituted nickel ferriteJournal of Magnetism and Magnetic Materials, 2015, 391, 195–202

[47] R.N. Panda, J.C. Shih, T.S. Chin, Magnetic properties of nano-crystalline Gd-or Pr-substituted $CoFe_2O_4$ synthesized by the citrate precursor technique, J. Magn. Magn.Mater. 2003, 257, 79.

[48]XiangqianLipingGuo, Fuzhan Shen, Lin Song, Yongwei Zhu Lin, Structure and magnetic property of $CoFe_{2-x}Sm_xO_4$ (x= 0–0.2) nanofibers prepared by sol–gel route , Mater. Chem. Phys., 2011, 129, 943-947

[49]Lija K. Joya, SenoyThomasb, M.R. Anantharamana, A study on the magnetic properties of Gd–Sr based low bandwidth manganites in their bulk and thin film forms and evidence for

magnetization reversal in bulk $Gd_{0.7}Sr_{0.3}MnO_3$, Journal of Magnetism and Magnetic Materials, 2016, 398, , 174–182

Graphical abstract

One of the most known applications of Lanthanum strontium manganite as a cathode materials in solid oxide fuel cells technology